BIOCHEMISTRY
including biophysical chemistry & molecular biology

ARTICLE

pubs.acs.org/biochemistry

Molecular Mechanism of Action of β-Hairpin Antimicrobial Peptide Arenicin: Oligomeric Structure in Dodecylphosphocholine Micelles and Pore Formation in Planar Lipid Bilayers

Zakhar O. Shenkarev, Sergey V. Balandin, Kirill I. Trunov, Alexander S. Paramonov, Stanislav V. Sukhanov, Leonid I. Barsukov, Alexander S. Arseniev, and Tatiana V. Ovchinnikova*

Shemyakin-Ovchinnikov Institute of Bioorganic Chemistry, Russian Academy of Sciences, 16/10 Miklukho-Maklaya strasse, Moscow 117997, Russia

Supporting Information

ABSTRACT: The membrane-active, cationic, β-hairpin peptide, arenicin, isolated from marine polychaeta *Arenicola marina* exhibits a broad spectrum of antimicrobial activity. The peptide in aqueous solution adopts the significantly twisted β-hairpin conformation without pronounced amphipathicity. To assess the mechanism of arenicin action, the spatial structure and backbone dynamics of the peptide in membrane-mimicking media and its pore-forming activity in planar lipid bilayers were studied. The spatial structure of the asymmetric arenicin dimer stabilized by parallel association of N-terminal strands of two β-hairpins was determined using triple-resonance nuclear magnetic resonance (NMR) spectroscopy in dodecylphosphocholine (DPC) micelles. Interaction of arenicin with micelles and its oligomerization significantly decreased the right-handed twist of the β-hairpin, increased its amphipathicity, and led to stabilization of the peptide backbone on a picosecond to nanosecond time scale. Relaxation enhancement induced by water-soluble (Mn^{2+}) and lipid-soluble (16-doxylstearate) paramagnetic probes pointed to the dimer transmembrane arrangement. Qualitative NMR and circular dichroism study of arenicin-2 in mixed DPC/1,2-dioleoyl-*sn*-glycero-3-phosphoglycerol bicelles, sodium dodecyl sulfate micelles, and lipid vesicles confirmed that a similar dimeric assembly of the peptide was retained in membrane-mimicking systems containing negatively charged lipids and detergents. Arenicin-induced conductance was dependent on the lipid composition of the membrane. Arenicin low-conductivity pores were detected in the phosphatidylethanolamine-containing lipid mixture, whereas the high-conductivity pores were observed in an exclusively anionic lipid system. The measured conductivity levels agreed with the model in which arenicin antimicrobial activity was mediated by the formation of toroidal pores assembled of two, three, or four β-structural peptide dimers and lipid molecules. The structural transitions involved in arenicin membrane-disruptive action are discussed.

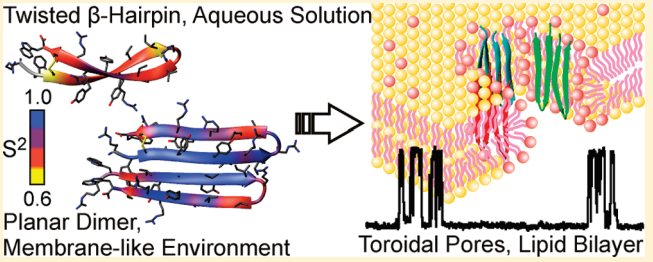

Cationic antimicrobial peptides (AMPs) constitute an important part of the host defense systems of multicellular organisms.[1] These broad-spectrum antibiotics kill bacterial and fungal cells via destabilization of their cytoplasmic membranes.[2] Structurally, the plethora of AMPs can be divided into several classes.[3] The most abundant of them are (i) the linear peptides forming amphiphatic α-helical structure when interacting with lipid bilayers (e.g., amphibian magainins, insect cecropins, and mammalian cathelicidins) and (ii) disulfide-stabilized peptides, including β-structural regions (e.g., plant, insect, and mammalian defensins).[3] The last ones include β-hairpin peptides, such as protegrins from porcine leucocytes,[4] tachyplesins, and polyphemusins from hemocytes of the horseshoe crab,[5] gomesin from hemocytes of the tarantula spider,[6] and androctonin from scorpion blood.[7]

Extensive studies of α-helical peptides revealed several putative mechanisms that explain a membrane-disruptive action of AMPs.[8,9] In the "barrel-stave" model, the peptides form pores in the cytoplasmic membrane of the target cell, leading to leakage of cell constituents and/or osmotic lysis.[10] The "toroidal pore" model implies the formation of mixed lipid/peptide pores with overall torus-like geometry.[11,12] On the other hand, within the "carpet model", the high density of monomeric or oligomeric peptides on the external membrane surface causes the extensive membrane curvature strain and leads to micellization and disintegration of the bilayer.[13] There is also a unifying model that describes different aspects of the detergent-like action of α-helical amphipathic peptides in terms of the phase diagram of the peptide/phospholipid mixture.[14] There are several structural transitions implied within these models. (i) An α-helical AMP frequently having a distorted structure in aqueous solution becomes more structured when contacting the lipid bilayer

Received: May 13, 2011
Revised: May 28, 2011
Published: June 01, 2011

surface. (ii) The peptide forms aggregate on the membrane surface or within the hydrophobic region of the bilayer. (iii) The monomeric or oligomeric AMP initially bound to the membrane surface accomplishes the transition into the transmembrane (TM)-inserted state to form pores.[15] At present, the question of the applicability of these mechanistic models to β-structural peptides remains open.

Earlier, we discovered two novel 21-residue antimicrobial peptides, termed arenicins, from coelomocytes of marine polychaeta lugworm *Arenicola marina*.[16] Both arenicin-1 (RWCVYAYVRVRGVLVRYRRCW, 2758.3 Da) and arenicin-2 (RWCVYAYVRIRGVLVRYRRCW, 2772.3 Da) exhibit potent activity against Gram-positive and Gram-negative bacteria and fungi. Each isoform has one disulfide bond (Cys3−Cys20) forming an 18-residue ring. Our previous investigation of the spatial structure of arenicin-2 in aqueous solution by ^{1}H NMR spectroscopy showed the peptide as a prolonged β-hairpin formed by two β-strands (Cys3−Ile10 and Val13−Cys20) and type I′ β-turn (Arg11−Gly12).[17] The two-stranded β-sheet in the arenicin-2 structure has a significant right-handed twist in aqueous solution. This distortion effectively shields the hydrophobic side of the β-sheet from contacts with polar solvent and deprives the peptide surface of amphipathicity. Qualitative ^{1}H NMR investigation of arenicin-2 in the membrane-mimicking environment of dodecylphosphocholine (DPC) micelles reveals the peptide specific dimerization by parallel association of its N-terminal strands.[18]

Here we report the results of structural studies of the arenicin-2 dimer in detergent-containing membrane-mimicking media and anionic lipid vesicles in combination with the data of electrochemical measurements of arenicin-induced ion conductance of planar lipid bilayers [bilayer lipid membrane (BLM)]. The obtained results are in good agreement with the toroidal pore model of arenicin action on bacterial membranes. Structural transitions involved in this action appear evident from the given results. These transitions include the peptide ordering and dimerization on contact with the anisotropic environment of a lipid membrane and lipid-mediated assembly of the peptide dimers in TM arrangement into oligomeric lipid/peptide pores of variable stoichiometry. The results presented here improved our understanding of the mechanism of cationic β-hairpin AMP action.

MATERIALS AND METHODS

Expression of Uniformly ^{15}N-Labeled and ^{13}C- and ^{15}N-Labeled Recombinant Arenicin-2. Recombinant arenicin-2 was expressed in the *Escherichia coli* BL-21(DE3) strain transformed with the pET-His8-TrxL-Ar2 plasmid constructed as described previously.[17] The expression cassette was composed of a T7 promoter, a ribosome binding site, and a sequence encoding the recombinant protein that included an octahistidine tag, the TrxL carrier protein (*E. coli* thioredoxin A with the M37L mutation), a methionine residue, and the mature arenicin-2. This sequence was ligated to the *Bgl*II/XhoI fragment of the pET-20b(+) vector (Merck KGaA, Darmstadt, Germany) containing the pBR322 origin of replication, a β-lactamase gene, and a T7 terminator. The transformants were grown in Lysogeny broth (LB) medium containing 100 mkg/mL ampicillin and 20 mM glucose at 37 °C to an OD_{600} of 2.0−3.0. The cells were washed several times with sterile phosphate buffer and then resuspended in a 10-fold volume of M9 minimal medium containing 1 g/L $^{15}NH_4Cl$ (CIL, Andover, MA). To obtain ^{13}C- and ^{15}N-labeled peptide, we substituted [$^{12}C_6$]glucose with [U-$^{13}C_6$]glucose (CIL). The cells grown to an OD_{600} of 0.7−1.0 were induced with 0.2 mM isopropyl β-D-1-thiogalactopyranoside at 25−30 °C and incubated at the same temperature in an orbital shaker for 16−18 h.

Purification of Recombinant Arenicin-2 Labeled with Stable Isotopes. This part of the protocol was identical for ^{15}N-labeled and ^{13}C- and ^{15}N-labeled peptides. The cells were harvested by centrifugation and sonicated in a buffer containing 100 mM Na_2HPO_4/NaH_2PO_4 (pH 7.8), 0.5 M NaCl, 1% Triton X-100, and 1 mM PMSF. The insoluble fraction was separated by centrifugation and then repeatedly washed with 25 mM phosphate buffer (pH 7.8). Inclusion bodies were solubilized (20−40 mg/mL) in 100 mM phosphate buffer (pH 7.8) containing 6 M guanidine hydrochloride and 10 mM imidazole and applied to a column packed with Ni-NTA agarose (Qiagen, Venlo, The Netherlands). The His8-tagged fusion protein was eluted with 0.5 M imidazole, dialyzed against water, dissolved in 80% TFA (20 mg/mL), and cleaved with an equal mass of CNBr under standard conditions. Lyophilized products of the cleavage reaction were redissolved in 80% TFA and loaded onto a reversed-phase HPLC semipreparative Reprosil-pur C18-AQ column (Dr. Maisch GmbH, Ammerbuch-Entringen, Germany). HPLC was performed with a linear gradient of acetonitrile in water containing 0.1% TFA. The peak of arenicin-2, identified by tris-tricine sodium dodecyl sulfate−polyacrylamide gel electrophoresis and MALDI-TOF MS, was concentrated in vacuo and repurified under the same HPLC conditions. TFA was removed during repetitive lyophilization. The rechromatographed peptide had a purity of at least 99% as measured by RP-HPLC, MALDI-TOF MS, and NMR.

NMR Experiments, Spatial Structure Calculation, and Analysis of Relaxation Data. The spatial structure and backbone dynamics of arenicin-2 were investigated using samples containing 0.4−1.2 mM unlabeled, ^{15}N-labeled, or ^{13}C- and ^{15}N-labeled peptide in 5 or 100% D_2O. For measurements in detergent micelles, d_{38}-DPC or d_{25}-SDS (CIL) was added to the peptide samples using aliquots of a concentrated solution in H_2O or D_2O. The titration of the arenicin/DPC sample with DOPG (Avanti Polar Lipids, Alabaster, AL) was conducted using a concentrated solution of the lipid in H_2O. Unless otherwise stated, the NMR spectra were recorded on Bruker Avance 800 and 600 spectrometers equipped with cryoprobes. ^{1}H, ^{13}C, and ^{15}N resonance assignments of the arenicin-2 dimer in complex with DPC micelles (pH 4.5 and 30 °C) were obtained by a standard procedure based on a combination of three-dimensional HNCO, HNCA, HNCACB, and H(C)CH-TOCSY spectra.[19] The $^3J_{H^N,H^\alpha}$ coupling constants were determined using amplitude-modulated ^{1}H−^{15}N TROSY spectra (see the experimental procedures in the Supporting Information). The $^3J_{H^\alpha,H^\beta}$ and $^3J_{H^\beta,H^\gamma}$ coupling constants were measured using ACME[20] in the COSY spectrum in a 100% D_2O solution (60 °C, room-temperature probe). The spatial structure was calculated using CYANA.[21] Upper interproton distance constraints were derived from cross-peaks observed in three-dimensional ^{15}N-separated (τ_m = 60 ms, 800 MHz) and ^{13}C-separated (τ_m = 50 ms, 100% D_2O, 600 MHz) NOESY spectra via a "$1/r^6$" calibration. Torsion angle restraints and stereospecific assignments were obtained from *J* coupling constants and NOE intensities. Hydrogen bonds were introduced on the basis of temperature coefficients and deuterium exchange rates of H^N protons (Figure S1 of the Supporting Information).

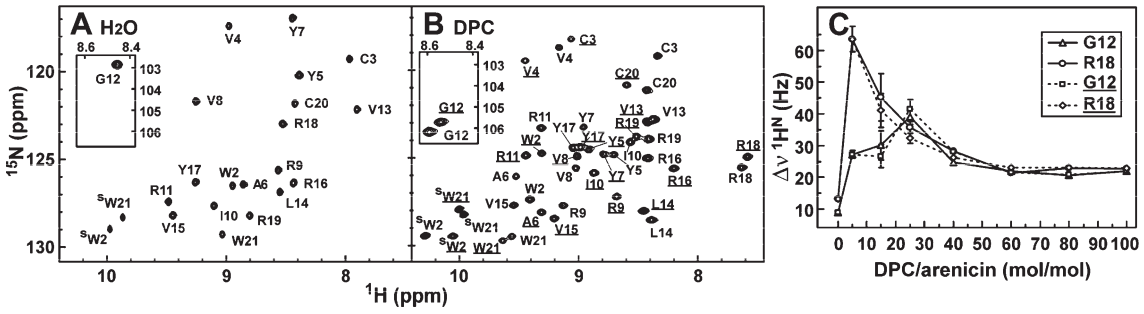

Figure 1. $^{1}H-^{15}N$ heteronuclear single-quantum coherence spectra of 1.2 mM arenicin-2 in aqueous solution (A) and in DPC micelles (B). The spectra were recorded at pH 4.5 and 43 °C. Spectrum B was recorded at an arenicin:DPC molar ratio of 1:100. The obtained resonance assignments are shown. The signals of monomer B in DPC micelles are underlined. The resonances of side chain groups are marked with a superscript s. (C) Dependence of the $^{1}H^{N}$ line widths of Gly12 and Arg18 on the detergent molar concentration. Data for both peptide monomers are shown.

The relaxation parameters of ^{15}N nuclei (R_1, R_2, and NOE) were measured at 800 MHz for arenicin-2 in water (pH 4.5, 30 °C) and in DPC micelles (pH 4.5, 43 °C) as described in ref 22. Chemical shift anisotropy/dipolar cross-correlation rates (η_{XY}) of ^{15}N nuclei were measured for arenicin-2 in DPC micelles using constant-time amplitude-modulated $^{1}H-^{15}N$ TROSY spectra.[23] The extent of microsecond to millisecond fluctuations in the peptide in complex with DPC micelles was qualitatively deduced using the R_1R_2 product as described in ref 24 (Figure S4 of the Supporting Information) and the plot of R_2 versus η_{XY} (Figure S5 of the Supporting Information). Model-free analysis of relaxation data was performed with FastModelFree[25] using an isotropic rotational model (Figure S4 of the Supporting Information). The paramagnetic probes 16-doxylstearate (16-DSA, Sigma) and Mn^{2+} (in the form of $MnCl_2$) were added to the arenicin/DPC sample using aliquots of stock solutions in methanol and H_2O, respectively. The paramagnetic enhancement of the transverse relaxation rate of H^N protons was quantified using $^{1}H-^{15}N$ TROSY spectra according to the method described in ref 26.

CD Spectroscopy. All CD spectra were recorded on a Jasco J-810 instrument at ambient temperature. Small unilamellar vesicles (SUV) were prepared via sonication. A solution of arenicin-2 in 10 mM Tris (pH 7.0) was added to vesicle or micelle suspensions in the same buffer for CD measurements. The lipid or detergent concentration in the samples was 15 mM, and the peptide concentration was 0.07−0.3 mM (see Figure 3E).

Preparation of Planar Bilayers and Electrochemical Measurements. The BLM mimicking the plasma membrane of Gram-negative bacteria (phospholipid mixture PL^{G-}) was made of polar lipid extract from *E. coli* (Avanti Polar Lipids) consisting of PE, PG, and DPG (cardiolipin) in a 67:23.2:9.8 ratio (weight percent). The BLM mimicking the plasma membrane of Gram-positive bacteria (phospholipid mixture PL^{G+}) was composed of DPG from *E. coli*, PG from *E. coli*, and soy L-α-phosphatidylinositol (all from Avanti Polar Lipids) at a 66:24:10 ratio (weight percent) using the phospholipid composition of the plasma membrane of the Gram-positive bacterium *Micrococcus lysodeikticus* (the current name is *Micrococcus luteus*) as a prototype.[27] BLMs were formed from a 5% lipid solution in *n*-decane by the Mueller technique[28] on a 0.85 mm orifice in a Teflon partition separating two compartments of 2 mL each. Arenicin-1 and arenicin-2 in the buffer were added to both compartments to final concentrations of 0.05−0.5 μM; these conditions were optimal for the observation of distinct conductivity levels appropriate for subsequent pore analysis. The measurements were taken in 5 mM HEPES and 0.67 M NaCl at pH 7.4 and 20 °C. The current records were digitized at a 10 kHz frequency and analyzed using ClampFit (version 9.2; Axon Instruments Inc.) and Mathematica (Wolfram research). Pore area (S^p) was calculated using the formula $S^p = L \times g/\sigma$, where L is the thickness of a membrane (50 Å), g is the measured conductance, and σ is the conductance of an electrolyte (5.21 S/m). Geometrical models of arenicin pores were fitted into the calculated S^p values using Mathematica.

RESULTS

Expression and Purification of Recombinant Arenicin-2 Labeled with Stable Isotopes. The labeled peptides were expressed in *E. coli* strain BL21(DE3) transformed by pET-His8-TrxL-Ar2, the same plasmid previously employed to prepare unlabeled arenicin-2.[17,18] In this system, the arenicin expression level is enhanced by thioredoxin fusion providing temporary neutralization of the target product toxicity and its protection from degradation in a heterologous environment. The transformed cells were cultivated in minimal medium containing either ^{15}N-labeled ammonium chloride or ^{15}N-labeled ammonium chloride and [U-$^{13}C_6$]glucose as the only nitrogen and carbon sources, respectively. The recombinant protein composed of the target peptide, thioredoxin A (M37L), and an N-terminal octahistidine tag was obtained mostly as insoluble matter. After Ni^{2+} affinity chromatography and specific CNBr cleavage of the fusion protein, the target peptide was purified through two consecutive steps of reversed-phase HPLC in a linear acetonitrile concentration gradient. The final yield was approximately 4 mg of ^{15}N-labeled arenicin-2 and 1 mg of ^{13}C- and ^{15}N-labeled arenicin-2 per liter of culture. Both purified ^{15}N-labeled and ^{13}C- and ^{15}N-labeled arenicin-2 were analyzed by MALDI-TOF MS. The experimentally measured m/z values of ^{15}N-labeled and ^{13}C- and ^{15}N-labeled arenicin-2 (2813.5 and 2940.5, respectively) matched well the $[M + H]^+$ values of the calculated molecular masses of the labeled peptides (2812.5 and 2939.5 Da, respectively).

Dimerization of Arenicin-2 in DPC Micelles. The formation of the complex between arenicin-2 and DPC micelles accompanied by peptide dimerization was studied by two-dimensional $^{1}H-^{15}N$ NMR spectroscopy (Figure 1A−C). Addition of the detergent to the peptide sample to a final detergent:peptide molar ratio (D:P) of 5 significantly broadened arenicin-2 signals.

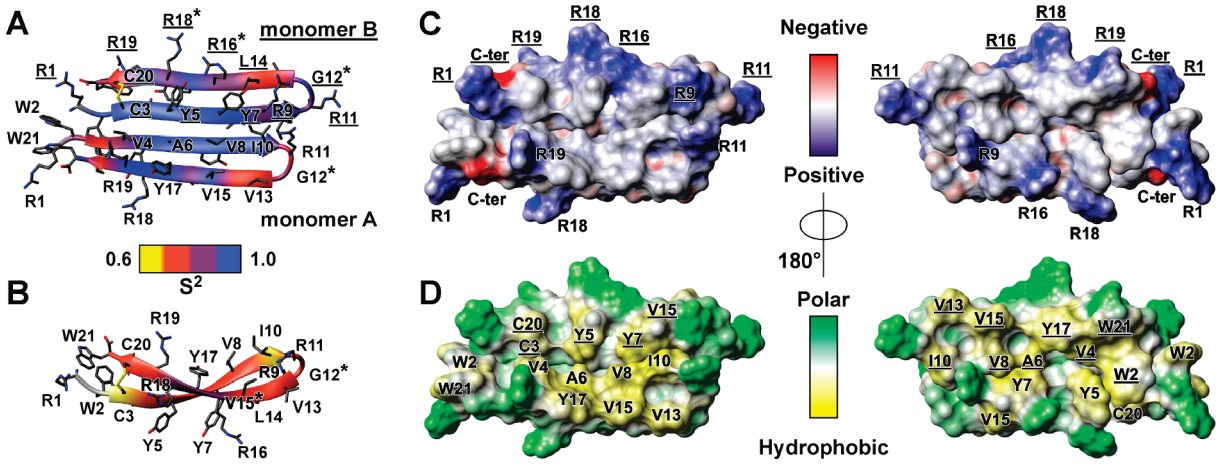

Figure 2. Spatial structure and backbone dynamics of the arenicin-2 dimer in complex with DPC micelles. (A) The peptide ribbon is colored according to obtained dynamical NMR data. The values of generalized order parameters (S^2) calculated during "model-free" analysis of ^{15}N relaxation data are color-coded. The residues affected by dynamic processes on the picosecond to nanosecond time scale demonstrate lower S^2 values. The residues affected by dynamic processes on the microsecond to millisecond time scale (having R_{EX} values of >2 Hz) are marked by asterisks. The two arenicin-2 monomers (A and B) are labeled. The labels for residues from monomer B are underlined. (B) Spatial structure and backbone dynamics of monomeric arenicin-2 in aqueous solution. The obtained dynamical NMR data are mapped on the previously determined spatial structure of the peptide (Protein Data Bank entry 2JNI) using the coloring scheme in panel A. (C and D) Two-sided view of electrostatic and molecular hydrophobicity[30] potentials on the arenicin-2 dimer surface. Red, blue, green, and yellow areas denote negative, positive, polar, and hydrophobic regions, respectively. This figure was prepared with MolMol.[31]

A further increase in D:P led to the appearance of a specific spectral pattern characterized by a double number of $^1H-^{15}N$ resonances and corresponded to the peptide dimer in complex with the DPC micelle. An increase in the detergent concentration also resulted in gradual narrowing of the peptide signals with the $^1H^N$ line width going into the plateau at D:P ratios of >40:1 (Figure 1C). The obtained data indicated that the observed signal broadening is a consequence of exchange process(es) between different structural states of the peptide (e.g., monomer, dimer, etc.) taking place on the microsecond to millisecond time scale. To minimize the influence of these processes, we conducted the structural study of arenicin-2 at a D:P of 100:1, where the peptide dimer represented the major structural state. Moderately acidic conditions (pH 4.5) were chosen for the NMR study. Arenicin-2 contains only one ionogenic group (the C-terminal carboxyl) that can be titrated under the acidic conditions. The pH titration experiments (see the Supporting Information) ensured that the peptide dimer in complex with DPC micelles had an identical spatial structure at moderately acidic pH and at neutral pH.

Spatial Structure of the Micelle-Bound Dimer of Arenicin-2. The spatial structure of the arenicin-2 dimer in complex with DPC micelle was determined by triple-resonance NMR spectroscopy. The summary of the obtained NMR data, a calculated set of 20 dimer structures, and structural statistics are shown in Figures S1 and S3 and Table S1 of the Supporting Information, respectively. The ribbon representation of the arenicin-2 dimer in the micelle-bound form is shown in Figure 2A. Each peptide monomer (A and B) represents the β-hairpin formed by two β-strands (Cys3−Ile10 and Val13−Cys20) and a type II′ β-turn (Arg11−Gly12). The spatial structure of each monomer is stabilized by nine intramolecular hydrogen bonds and one disulfide bridge (Cys3−Cys20), having a "short right-handed hook" or *g*+*npng*+ conformation (see the Supporting Information for the definition). The asymmetric dimer is formed by parallel association of N-terminal β-strands (CN↑↑NC type of association), with the monomer B shifted by one residue relative to monomer A. The dimer is stabilized by seven intermolecular hydrogen bonds, involving HN groups of Cys3, Tyr5, Tyr7, and Arg9 from monomer A and Cys3, Tyr5, and Tyr7 from monomer B (Figure S1 of the Supporting Information). As a result of this asymmetry, the monomers demonstrate slightly different spatial structures.

According to previous NMR and molecular dynamic investigations, the β-hairpin of arenicin-2 in aqueous solution is significantly kinked and twisted[17,29] (Figure 2B). In a water environment, the β-hairpin had a kink angle of ~35° and a right-handed twist of ~200° (per eight residues). In contrast to that, the four-stranded β-structural dimer of arenicin-2 in a solution of DPC micelles is significantly more planar. In the NMR-derived set of structures, monomers A and B are characterized by kink angles of 6 ± 2° and 12 ± 2° and by right-handed twists of 52 ± 9° and 29 ± 9°, respectively. Interestingly, a larger kink of monomer B, as compared to monomer A, is compensated by a smaller value of the twist angle. As a result, a relatively flat dimer of arenicin-2 has a platelike overall shape and resembles a parallelogram with sides of ~36 and ~20 Å, and a thickness of ~14 Å (including side chains). Noteworthy is the fact that the longest "diagonal" of this parallelogram (distance between the Trp21 side chain of monomer A and Arg11 of monomer B) is ~47 Å long.

The interaction interface within the dimer (Cys3−Ile10 of monomer A and Trp2−Arg9 of monomer B) involves mainly aromatic and hydrophobic residues, and all charged groups [N-terminal amines, guanidine groups of 12 Arg residues (six per monomer), and C-terminal carboxyl groups] became segregated at the rim of the dimer "plate". The maps of electrostatic (Figure 2C) and molecular hydrophobicity (Figure 2D) potentials on the surface of the arenicin-2 dimer illustrate its amphipathic nature. The two almost symmetrical hydrophobic patches on the dimer surface are formed in the middle of both sides of the plate by the aromatic and hydrophobic side chains from the

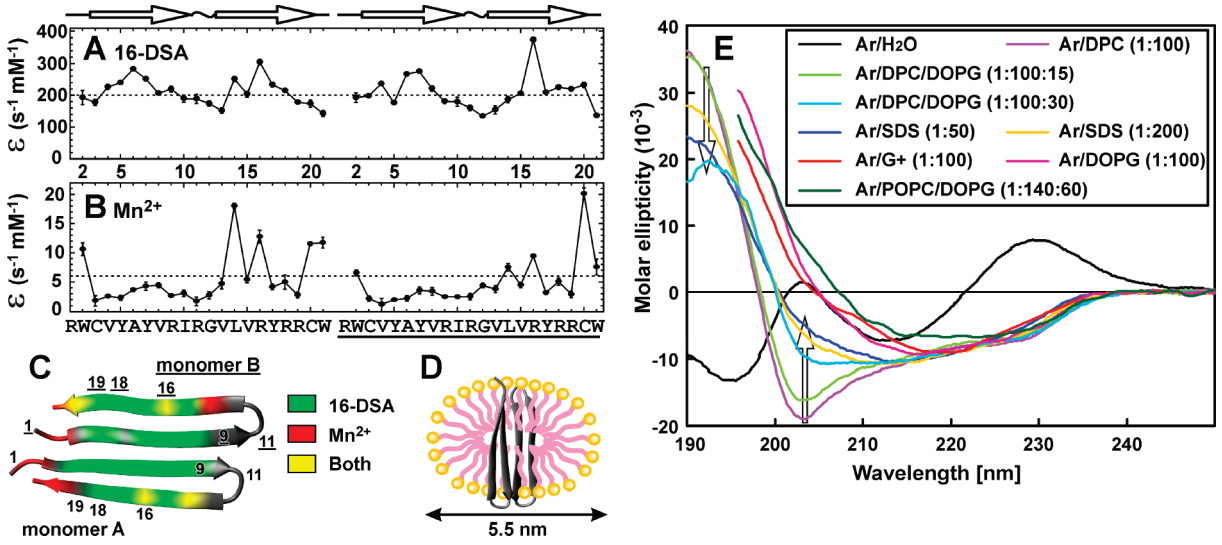

Figure 3. (A and B) Paramagnetic enhancement (ε) of the transverse relaxation rate of H^N protons of the arenicin-2 dimer in complex with DPC micelles induced by (A) lipid-soluble 16-DSA and (B) water-soluble $MnCl_2$. The 200 s^{-1} mM^{-1} threshold line in panel A subdivides data points in two groups: the residues located inside or outside the hydrophobic region of the micelle. The residues displaying an ε of >6 s^{-1} mM^{-1} in panel B are possibly located in the vicinity with phosphate groups of the detergent. (C) Data mapped on the structure of the arenicin-2 dimer. For residues colored green, red, and yellow, ε values above the given thresholds for 16-DSA, Mn^{2+}, and both paramagnetic probes, respectively, were observed. For residues colored gray, the determined ε values were below the given thresholds. The positions of Arg residues are labeled. The labels for residues from monomer B are underlined. (D) Proposed topology of the arenicin-2/DPC complex. (E) CD spectra of arenicin-2 (Ar) in water, detergent micelles, detergent/lipid bicelles, and lipid vesicles. The composition of the membrane-mimicking medium and the peptide:lipid ratio are given in the legend. Arrows indicate the variable intensities of bands at ~195 and 203 nm for the samples that contain the arenicin-2 dimers according to NMR analysis. The spectra in vesicles are presented only from 197 nm to exclude distortions induced by light scattering.

N-terminal β-strands and by the Val13, Val15, and Tyr17 side chains from the C-terminal strands of both the β-hairpins. The distribution of hydrophobic and polar groups on the surface of the arenicin-2 dimer observed in DPC micelles is dissimilar to that of the monomeric peptide in aqueous solution, where a large twist of the β-hairpin (Figure 2B) effectively prevents formation of large hydrophobic patches on the peptide surface.[17]

Backbone Dynamics of Arenicin-2 in Aqueous Solution and a DPC Micelle Environment. To track the changes in the dynamics of the arenicin-2 backbone upon interaction with DPC micelles and dimerization, the ^{15}N relaxation parameters (R_1 and R_2 relaxation rates and heteronuclear $^{15}N-\{^1H\}$ NOEs) were measured at 800 MHz for monomeric arenicin-2 in aqueous solution and for the peptide dimer in complex with DPC micelles (Figure S4 of the Supporting Information). The relaxation data were analyzed by the so-called model-free approach (see the review in ref 22) providing information about intramolecular motions on two time scales (picoseconds to nanoseconds and microseconds to milliseconds). Mapping of the obtained values of the generalized order parameter (S^2) on the structures of the arenicin-2 dimer and monomer (Figure 2A,B) revealed that in both cases the central regions of β-strands are more stable on the picosecond to nanosecond time scale than N- and C-terminal fragments and the fragments encompassing β-turns. Nevertheless, the overall stability of the peptide backbone in two milieus is markedly different. The increase in the average S^2 value from 0.76 $\pm$ 0.4 to 0.88 $\pm$ 0.7 pointed to significant stabilization of the arenicin-2 backbone on the picosecond to nanosecond time scale upon incorporation into DPC micelles and dimerization. Interestingly, the lowest mobility on this time scale was observed for the residues located in the interaction interface within the dimer.

In contrast to the observed dissimilarity in picosecond to nanosecond dynamics, arenicin-2 demonstrates a quite similar distribution of microsecond to millisecond conformational fluctuations in aqueous solution and in DPC micelles (Figure 2A,B and Figure S4 of the Supporting Information). The largest (>8 Hz) exchange contribution to the ^{15}N transverse relaxation rate (R_{EX}) was detected in both cases for $^{15}N^H$ nuclei of Gly12. In addition, small, but significant, R_{EX} contributions (>2 Hz) were detected for the residues from C-terminal strands of β-hairpins (Val15 in water and Arg16 and Arg18 from monomer B in DPC). The observation of microsecond to millisecond conformational fluctuations at Gly12 supplements previous data on the molecular dynamic study of arenicin-2 in aqueous solution where the dynamic fluctuations of the β-turn conformation were observed.[29] Most probably, the β-turn motif within the peptide is able to switch between several conformations both in water and in DPC micelles. Moreover, according to NMR data, the most populated state of the β-turn depends on the environment and represents type I′ in water and type II′ in DPC micelles. The absence of a detectable R_{EX} contribution at the residues adjacent to Gly12 could be explained by a slight variation in their $^{15}N^H$ chemical shifts upon β-turn fluctuations that involve changes of only two backbone angles, ψ of Arg11 and φ of Gly12.

Stoichiometry and Topology of the Arenicin-2/DPC Micelle Complex. The model-free analysis of ^{15}N relaxation data also provides information about rotational diffusion of macromolecules in solution. The determined overall rotational correlation times (τ_R) of ~1.5 ns (water, 30 °C) and 12.6 ns (DPC micelles, 43 °C) are consistent with reorientation of the monomeric peptide and relatively large peptide−detergent complex, having hydrodynamic Stokes radii (R_H) of ~12.3 and ~27.7 Å, and apparent molecular masses of ~3 and ~33 kDa, respectively.

dx.doi.org/10.1021/bi200746t |*Biochemistry* 2011, 50, 6255–6265

A similar average τ_R value (12.4 ± 1.3 ns) was calculated for the arenicin-2 dimer in complex with DPC micelles from measured ^{15}N η_{XY} rates [16.3 ± 1.8 s^{-1} (Figure S4 of the Supporting Information)] by the approach described in ref 32. The estimated mass of the mixed arenicin-2/DPC micelle (~33 kDa) roughly corresponds to that of the peptide dimer (~5.5 kDa) in complex with 80 DPC molecules (~28 kDa). This stoichiometry (2:80) is consistent with the DPC titration data (Figure 1C), where no significant changes in $^1H^N$ line widths of the peptide were observed at a D:P ratio of >40:1.

The topology of the arenicin-2/DPC complex was elucidated using two paramagnetic probes, 16-DSA and Mn^{2+} ,with different localization within the micelle. The paramagnetic nitroxide moiety of 16-DSA is preferentially located close to the micelle center.[33] On the other hand, divalent Mn^{2+} cations have affinity for negatively charged phosphate groups of the detergent[34] (arenicin-2 has only one negatively charged group, the C-terminal carboxyl). The paramagnetic relaxation enhancement induced by 16-DSA revealed that the central regions of the four β-strands of the dimer are embedded into the micelle interior (Figure 3A,C). On the other hand, Mn^{2+} ions effectively enhance the relaxation of protons from N- and C-terminal regions and from Leu14 and Arg16 residues belonging to the outer (C-terminal) β-strands (Figure 3B,C). Data obtained are consistent with the TM arrangement of the arenicin-2 dimer within the DPC micelle with the terminal regions and β-turn fragments of both the monomers located above the hydrophobic region of the micelle (Figure 3D). Nevertheless, observation of the strong simultaneous paramagnetic relaxation enhancement induced by 16-DSA and Mn^{2+} at the Arg16 residues indicates that within the arenicin-2/DPC complex the detergent headgroups can bend toward positively charged side chains located at the center of C-terminal β-strands of the dimer. Thus, the arenicin-2/DPC complex could be envisaged as a prolate ellipsoid, in which two hydrophobic surfaces of the dimer plate are covered by the hemispheres of detergent (Figure 3D).

Qualitative NMR Analysis of the Arenicin-2 Dimer in Membrane Mimetics Containing Anionic Lipids or Detergents. To investigate the influence of negatively charged lipid molecules on the structure of the peptide dimer, we titrated the previously prepared arenicin-2 (0.3 mM)/DPC (30 mM) sample with a concentrated water solution of anionic lipid DOPG. The $^1H-^{15}N$ TROSY spectrum measured at an arenicin-2:DPC:DOPG molar ratio of 1:100:15 revealed that the dimer preserves its spatial organization (Figure S6A of the Supporting Information). The overall rotational correlation time of the arenicin/DPC/DOPG mixed micelle was estimated from the measured η_{XY} rates [38.8 ± 6.6 s^{-1} (Figure S6D of the Supporting Information)]. The obtained τ_R value (25.5 ± 5.2 ns) corresponds to reorientation of a globular particle with an R_H of 35.0 ± 2.2 Å and an apparent mass of 67 ± 14 kDa. Comparison of the obtained values with the properties of the arenicin-2/DPC complex (see above) indicates that all added DOPG molecules (MW_{DOPG} = 797 Da) are incorporated into the complex. At the same time, the incorporation of additional copies of the peptide dimers or DPC molecules is not excluded.

Most probable sites of interaction between the anionic lipid and the peptide dimer are positively charged guanidine groups of the Arg residues. Interestingly, addition of DOPG did not induce large changes in the chemical shifts of side chain HN^{ε} groups of Arg residues (Figure S6 of the Supporting Information). Thus, the chemical environment around the Arg side chains does not change much if DOPG is added to DPC. Most probably, guanidine groups of the peptide in DPC micelles are involved in electrostatic interactions with detergent negatively charged phosphate groups. In spite of that, the noticeable changes in the chemical shifts of backbone HN groups upon addition of DOPG were detected for residues Ala6, Val8, Val15, and Tyr17 located in the central region of all four β-strands of the dimer in the vicinity of Arg16 (Figure S6C of the Supporting Information). This observation points to the presence of energetically favorable interactions between phosphate groups of the lipid and guanidine groups of Arg side chains from the C-terminal β-strands of the dimer.

A subsequent increase in the DOPG concentration to a final arenicin-2:DPC:DOPG molar ratio of 1:100:30 initiated further growth in the mass of the arenicin-containing complexes. The $^1H-^{15}N$ CRINEPT spectrum measured under these conditions revealed a spectral pattern characteristic of the arenicin-2 dimer, but with $^1H^N$ line widths of ~70 Hz (Figure S6B of the Supporting Information). This indicates the formation of large particles with masses of ~100 kDa, which could contain more than one copy of the arenicin-2 dimer.

To characterize the structure of arenicin-2 in the environment of anionic detergents, SDS was added to the peptide sample in water. Like the situation observed with DPC, significant broadening of NMR signals of the peptide was observed when the detergent was added (data not shown). The tractable $^1H-^{15}N$ correlation NMR spectra of arenicin-2 were obtained only at a D:P of 200:1 (Figure S7 of the Supporting Information). Analysis of these spectra revealed that under these experimental conditions the peptide forms asymmetric dimers with a structure similar to that observed in DPC micelles. Noteworthy is the fact that a comparison of the arenicin-2 CD spectra measured in SDS micelles at D:P values of 200:1 and 50:1 revealed a quite similar conformation of the peptide (see below).

CD Spectroscopy in Lipid Vesicles. To investigate the arenicin-2 conformation in lipid bilayers, we recorded the CD spectra of the peptide in the presence of small unilamellar vesicles (SUV). As shown earlier, the peptide does not interact with vesicles formed exclusively from zwitterionic lipids (POPC).[17] Thus, the anionic or partially anionic lipid systems (DOPG, 7:3 POPC/DOPG, PL^{G+}, and PL^{G-} phospholipid mixtures) were chosen for CD investigation. The CD spectra of arenicin in SUV were compared with those measured in aqueous solution and in detergent-based DPC, DPC/DOPG, and SDS membrane mimetics. The results (Figure 3E) indicate that the CD spectrum of arenicin-2 undergoes dramatic changes upon the transition of the peptide from aqueous solution to the anisotropic environment of the lipid bilayer. The spectrum of the "atypical" view containing two positive (at ~203 and ~230 nm) and two negative (at ~195 and ~213 nm) bands was transformed to the spectrum with a view similar to canonical spectra of β-structure demonstrating only two bands (positive at ~195 nm and negative at ~220 nm). Very similar spectra were obtained in all the tested lipid systems (Figure 3E) except for the PE-containing PL^{G-} phospholipid mixture mimicking the plasma membrane of Gram-negative bacteria. As shown previously,[17] an addition of arenicin-2 to the vesicles containing ~70% PE led to fast and irreversible precipitation of the lipids. In this case, measurement of CD spectra became impossible because of significant light scattering. Interestingly, the other lipid systems also demonstrated different stability when the peptide was added. The SUV composed of exclusively anionic lipids (DOPG and PL^{G+}) were more stable,

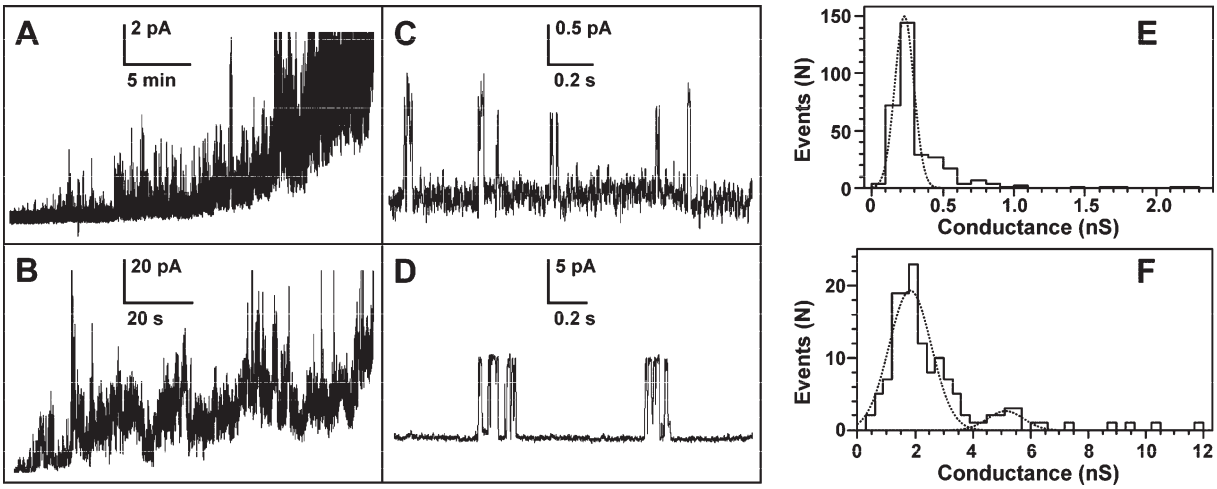

Figure 4. Permeabilization of planar lipid membranes by arenicin-1. The macroscopic peptide-induced current traces (A and B), the current traces of individual arenicin pores (C and D), and histograms of arenicin-induced conductance (E and F) are shown for BLMs composed of PL^{G-} (A, C, and E) and PL^{G+} (B, D, and F) phospholipid mixtures. In all cases, arenicin was added to both sides of BLM, the peptide concentration was 0.5 μM, the applied voltage was 50 mV, and the buffer solution consisted of 5 mM HEPES and 0.67 M NaCl (pH 7.4). The conductance histograms were fit using Gaussian functions (dashed).

permitting an addition of the peptide to the final peptide:lipid molar ratio of 1:100 without significant aggregation. At the same time, partially anionic SUV containing 70% zwitterionic lipid (7:3 POPC/DOPG mixture) were stable only at peptide:lipid ratios of <1:200.

The CD spectra of arenicin-2 measured in detergent-based membrane mimetics are also dissimilar to the spectrum of arenicin-2 in aqueous solution. In comparison with the spectra observed in SUV, they demonstrated an additional negative band at ~203 nm. The amplitude of the band significantly depended on the detergent composition of the sample. The lowest intensity of the band was observed for arenicin-2/DPC/DOPG (1:100:30) and arenicin-2/SDS (1:50 and 1:200) samples (Figure 3E). Bearing in mind that in all studied detergent-based membrane mimetics arenicin-2 adopts the β-structural dimer conformation, we can conclude that the peptide has a similar spatial structure in the vesicles of anionic lipids. The differences in CD intensity at ~203 nm can be attributed either to the contribution of the monomeric peptide population in solution (which demonstrates a positive band at this wavelength) or to CD bands corresponding to aromatic side chains of Tyr/Trp residues,[35] which could be differently oriented in detergent micelles and lipid membranes.

Arenicin-Induced Conductance of Planar Lipid Membranes. BLMs of two different lipid compositions were used to model an arenicin action on plasma membranes of Gram-negative and Gram-positive bacteria. The BLM-mimicking plasma membrane of Gram-negative bacteria (PL^{G-}) was formed using the phospholipid mixture consisting of ~70% zwitterionic PE and ~30% anionic PG and DPG (weight percent), whereas only anionic phospholipids DPG, PG, and phosphatidylinositol were used to prepare BLM-mimicking plasma membrane of Gram-positive bacteria (PL^{G+}). No significant differences were observed in BLM permeabilization induced by arenicin-1 and arenicin-2. Because a major part of the BLM measurements were taken with arenicin-1, the experimental data presented in Figure 4 are given for this peptide. Arenicins induce in both BLMs current fluctuations of steadily growing intensity (Figure 4A,B), resulting eventually in membrane rupture. The interaction of the peptide with PL^{G+} membranes occurs more rapidly with larger current fluctuations appearing immediately after the addition of the peptide (Figure 4B). On the other hand, the development of large-amplitude currents in PL^{G-} BLMs takes more time (Figure 4A). Inspection of electric recordings on an expanded time base reveals single-pore activities induced by arenicin (Figure 4C,D). In both cases, the pores have a similar average lifetime (44.3 ± 2.4 and 35.9 ± 1.0 ms for PL^{G-} and PL^{G+}, respectively), but they differ significantly in conductance levels (Figure 4E,F). The low-conductivity arenicin pores (~0.23 nS) were observed for the PL^{G-} mixture, whereas the pores of higher conductivity (~1.8 nS) were detected for the PL^{G+} BLM. Presuming cylindrical geometry of arenicin pore, one can calculate that these conductance levels correspond to buffer-filled annuli in the lipid membrane with areas (S^P) of ~22 and ~177 Å^2 and effective diameters (D^P) of ~5.3 and ~15.0 Å, respectively. Interestingly, the currents of a larger amplitude (~5.1 nS), corresponding to an S^P of ~494 Å^2 and a D^P of ~25.1 Å, were also rather frequently observed in PL^{G+} membranes (Figure 4F). Noteworthy is the fact that arenicin-1 conductivity levels (1.8/5.1 nS, 0.67 M NaCl) observed here for the PL^{G+} membranes roughly correspond to the levels (0.31/1.0 nS, 100 mM KCl) previously detected for arenicin-1 in the BLMs with different lipid compositions.[36] In addition, quite recently, arenicin-induced defined conductivity levels were also observed in BLM consisting of PG, lysyl-PG, and PE (25:25:50).[37] At the same time, the low-conductivity arenicin pores observed in PL^{G-} membranes were not previously described.

DISCUSSION

The β-hairpin AMP arenicin has efficient and broad-spectrum antimicrobial activity probably mediated by the action of the peptide on cellular membranes.[17,38] Molecular mechanisms of the peptide−lipid interactions, disruption, and/or translocation across target membranes are still obscure. This study is focused on several structural aspects of arenicin membrane-mediated action: (i) changes in the peptide conformation and dynamics when contacting the lipid-mimicking environment, (ii) detailed

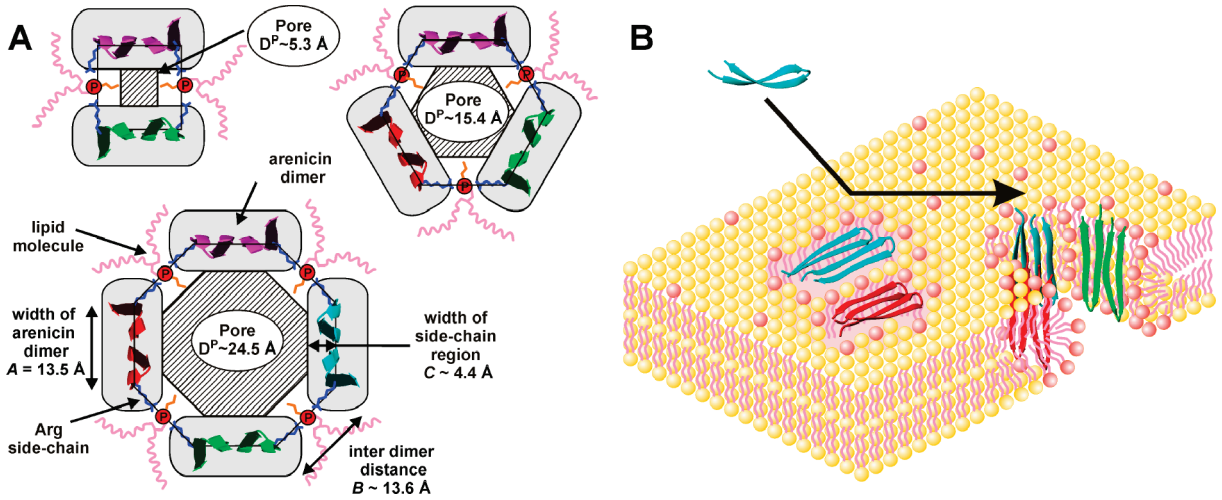

Figure 5. Mechanistic models of the toroidal pores formed by two, three, and four arenicin dimers (A) and proposed mechanism of arenicin membrane-disruptive action (B). The dimer and monomer of the peptide are shown in ribbon representation using NMR-derived coordinates (Protein Data Bank entries 2JNI and 2L8X, respectively). Different dimers within the pore assembly are variously colored. The best-fit geometric parameters of the pore models together with the predicted effective pore diameters (D^P) are shown in panel A.

membrane-bound peptide dimer structure, and (iii) molecular insight into formation of the peptide pore within membranes.

The solution of DPC micelles was chosen as the membrane-mimicking environment for the NMR study of arenicin-2. This relatively mild zwitterionic detergent was successfully used in numerous investigations of membrane proteins and membrane-active peptides. In most cases, it supported the membrane-relevant spatial structure of solubilized proteins and peptides,[39] although it is worth noting that in contrast to neutral DPC micelles, the bacterial membranes contain mainly anionic lipids and are negatively charged. Dimerization of the arenicin-2 in DPC micelles was recently observed by ^{1}H NMR spectroscopy.[18] The advances provided by recombinant peptide production, stable isotope labeling, and triple-resonance NMR spectroscopy contributed to determination of a high-resolution spatial structure of the arenicin-2 dimer in complex with DPC micelles (Figure 2). Comparison of data obtained with the results from a previous NMR study of monomeric arenicin-2 in aqueous solution[17] showed that interaction with micelles and oligomerization preserve the peptide secondary structure but significantly decrease the β-hairpin twist, markedly increase its amphipathicity, and lower the amplitude of picosecond to nanosecond time scale motions in the peptide backbone. It should be noted that amphipathicity of the peptide surface is one of the essential prerequisites for potent membrane activity.[1,3] Thus, the results indicate that the β-hairpin of arenicin has a propensity to adapt its structure to form energetically favorable interactions with the anisotropic membrane-mimicking environment. At the same time, it should be noted that the membrane-associated form of the β-hairpin peptide could also demonstrate some degree of intramolecular mobility. For example, the recent solid-state NMR study of arenicin detected significant conformational heterogeneity within the membrane-bound peptide.[40] This observation is consistent with microsecond to millisecond conformational fluctuations detected in the arenicin/DPC complex.

Similar behavior has been widely documented for α-helical AMPs, which frequently have no defined spatial structure in aqueous solution but form ordered amphipathic α-helices when contacting the lipid bilayer surface.[41] Interestingly, in some cases, oligomerization of α-helical AMPs in the membrane-mimicking environment of detergent micelles or lipid vesicles was observed by NMR spectroscopy.[42,43] On the other hand, data available for β-hairpin AMPs are scarce and contradictory. The high-resolution NMR study of tachyplesin I revealed substantial distortions in the hairpin structure induced by transition of the peptide from water to DPC micelles.[44] At the same time, during solid-state NMR investigation of tachyplesin in DMPC bilayers, the deviations from regular β-hairpin conformation were not detected.[45] In agreement with the latter finding, a solution NMR study of the closely related peptide polyphemusin (the synthetic analogue PV5) conducted in water and in DPC micelles did not reveal significant changes in the peptide backbone structure.[46] However, an increase in the amphipathicity of polyphemusin PV5 induced by reorganization of side chains was observed in DPC micelles.[46] The oligomerization of the β-hairpin AMPs was previously described only for protegrin I, for which the formation of asymmetric β-structural dimers stabilized by parallel association of C-terminal strands was observed by solid-state NMR spectroscopy in lipid bilayers.[47] Noteworthy is the fact that the oligomerization pattern of protegrin differs from that currently described for arenicin, which forms dimers by parallel association of N-terminal strands.

In earlier arenicin investigations, the peptide was supposed to form higher-order oligomers (tetramers, hexamers, octamers, etc.) in the membrane-mimicking environment containing negatively charged lipids or detergents.[18] Presently obtained NMR data collected in SDS micelles and DPC/DOPG bicelles (Figure S6 of the Supporting Information) were insufficient to confirm or disprove the formation of higher-order aggregates of the peptide in anionic or partially anionic media. Nevertheless, in combination with the results of CD spectroscopic investigation of arenicin-2 in lipid vesicles (Figure 3E), data obtained allowed us to propose that the main building block of these higher-order aggregates (if they exist) is represented by the peptide dimers having a structure similar to that observed in DPC micelles. Mn^{2+} and DOPG titrations (Figure 3B and Figure S6C of the Supporting Information) pointed to the presence of electrostatic interactions between Arg16 side chains located in the outer (C-terminal)

strands of the dimer and anionic phosphate groups of the lipid and/or detergent. Presumably, higher-order aggregates of arenicin-2 can be formed by loose association of the C-terminal β-strands of the dimers and stabilized by the lipid headgroups intercalating between them.

The insertion of the peptide into the hydrophobic core of the DPC micelle (Figure 3D) and geometric parameters of the dimer, having a length of ~35 Å sufficient to span the hydrophobic region of the bilayer, imply that the arenicin-2 dimer can adopt a TM orientation within the lipid membrane. Association of these TM dimers, in turn, can lead to formation of ion-conducting pores in the target bilayer. The obtained picture of possible arenicin-2 higher-order oligomerization in an anionic membrane-mimicking environment is consistent with only the toroidal pore mechanism of AMP action, where ion-conducting pores within the membrane are formed when lipid molecules are involved (Figure 5).

To test the conformance of the toroidal pore mechanism with the arenicin conductance levels observed in BLM systems, three mechanistic pore models were constructed (Figure 5A). These models involve two, three, and four arenicin dimers separated by lipid headgroups that intercalate between Arg side chains. The pore area (S^P) was calculated for each model as the area of the polygon (Figure 5A, cross-hatched) with the sides equal to the dimer width (A) and the distance between neighboring dimers (B) excluding the area occupied by the peptide side chains and lipid headgroups (equal length C was assumed). The models contain two variable parameters, B and C, and the width of the dimer (A, $C^\alpha - C^\alpha$ distance for the four-stranded β-sheet) was restricted to 13.5 Å. The fitting of pore areas predicted by these models to S^P values calculated from arenicin conductance levels allowed us to reproduce the pore area (and consequently conductivity levels) with errors no larger than 5%, giving values for the effective pore diameter (D^P) of ~5.3, ~15.4, and ~24.5 Å. The best-fit value of C (4.4 Å) is compatible with average lengths of amino acid side chains and lipid headgroups. Moreover, the calculated best-fit value of B (13.6 Å) agrees well with the distance expected between backbone atoms of two Arg residues with guanidine groups that form the hydrogen bonds with the phosphate of a lipid molecule assuming noncollinear geometry. Compatible dimer−dimer and guanidine−phosphate distances were observed for protegrin I in anionic PE/PG lipid bilayers, where according to solid state NMR data the dimers of protegrin form toroidal-like oligomers.[48]

Summarizing the discussion given above, we can conclude that electrochemical measurements in planar lipid bilayers are consistent with the toroidal pore mechanism of arenicin-2 action, and the peptide dimer represents the main structural unit involved in pore formation. The dithering of conductivity levels observed on the conductance histograms (Figure 4E,F) can occur as a consequence of the highly dynamic and fluctuating nature of the peptide/lipid assembles, having no stable contacts between the peptide dimers, and accommodate various distortions from ideal geometry. In this case, the proposed mechanistic models of tetrameric, hexameric, and octameric arenicin pores (Figure 5A) provide an average picture of the peptide/lipid assembles. In contrast to that the barrel-stave model of AMP, pore formation is not consistent with obtained permeability data. The stable peptide/peptide contacts implied within this model should lead to well-defined conductance levels with different spacing between them.[49]

Using available structural data, we can describe several structural transitions involved in arenicin membrane-disruptive action (Figure 5B). Initially, the peptide monomers, having the twisted β-hairpin conformation and enhanced intramolecular mobility, approach the anionic membrane surface. The peripheral binding to the bilayer induces dimerization of the peptide and diminishes an amplitude of intramolecular motions, which lead to the formation of amphipathic structure with the hydrophobic β-structural core and positively charged residues on its edge. The subsequent transition of the peptide dimers into the TM orientation leads to formation of ion-conducting pores in the target membrane according to the toroidal pore mechanism. Noteworthy is the fact that the surface-bound state of arenicin (Figure 5B) is not evident from the presently obtained structural data. Nevertheless, the presence of this structural state is supported by different stability of vesicular lipid systems upon addition of arenicin. Most probably, low charge density in the partially anionic POPC/DOPG (7:3) SUV makes stabilization of all bound peptide molecules in the TM arrangement impossible, and the peptide fraction remains surface-bound. This leads to electrostatic attraction between different vesicles and finally induces the precipitation of large peptide/lipid complexes. In this case, the replacement of zwitterionic phosphatidylcholine lipid with phosphatidylethanolamine should additionally stabilize the surface-bound state by invoking the significant negative curvature strain in the membrane.[50] In accordance with these expectations, the SUV containing ~70% PE [PL^{G-} mixture (this study) and 7:3 POPE/DOPG mixture[17]] demonstrated very low stability upon addition of arenicin. Low charge density and negative curvature strain induced by PE are probably responsible for low-conductivity arenicin pores in the PL^{G-} planar bilayers. The TM peptide density in this system could be too low for the formation of high-molecular mass aggregates and consequently high-conductivity pores observed in PL^{G+} BLMs. Noteworthy is the fact that the solid-state NMR study of arenicin also pointed to the presence of an equilibrium between TM and surface-bound structural states of the peptide.[40] Interestingly, the changes in peptide alignment in response to differences in lipid bilayer composition (surface-bound in POPE/POPG and TM in POPC) were recently observed by solid-state NMR for the fungal α-helical AMP alamethicin,[51] which acts according to the barrel-stave mechanism.[49]

In summary, this investigation provides the first high-resolution structure of dimeric β-hairpin AMP in a membrane-mimicking environment and gives a detailed description of changes in the structure and dynamics of the peptide upon interaction with the anisotropic membrane environment and dimerization. The electrochemical measurements in planar lipid membranes promoted for the fist time detection of low-conductivity arenicin pores, whereas structural data propose the toroidal pore mechanism of arenicin action.

■ ASSOCIATED CONTENT

Supporting Information. Experimental procedures, NMR spectra, J coupling constants, statistics of spatial structure calculation, ^{15}N relaxation rates, and results of model-free analysis. This material is available free of charge via the Internet at http://pubs.acs.org.

Accession Codes

The atomic coordinates and structure factors have been deposited in the Protein Data Bank as entry 2L8X.

AUTHOR INFORMATION

Corresponding Author

*Phone: +7(495)3364444. Fax: +7-495-336-43-33. E-mail: ovch@ibch.ru.

Funding Sources

The work was supported by the Russian Foundation for Basic Research (Grants 09-04-01202 and 10-04-01752), the Russian Federal Target Program "Scientific and Science-Educational Personnel of Innovative Russia" (Project NK-602P/19, State Contract P1159), a grant from the President of the Russian Federation (MK 8404.2010.4), and the Russian Academy of Sciences (Program "Molecular and Cellular Biology").

ABBREVIATIONS

16-DSA, 16-doxylstearate; η_{XY}, chemical shift anisotropy/dipolar cross-correlation rate; τ_R, effective rotational correlation time; AMP, antimicrobial peptide; BLM, bilayer lipid membrane; DOPG, 1,2-dioleoyl-*sn*-glycero-3-phosphoglycerol; DPC, dodecylphosphocholine; DPG, diphosphatidylglycerol (cardiolipin); D:P, detergent:peptide molar ratio; POPC, 1-palmitoyl-2-oleoyl-*sn*-glycero-3-phosphocholine; PC, phosphatidylcholine; PE, phosphatidylethanolamine; PG, phosphatidylglycerol; PL^{G-}, phospholipid mixture mimicking the plasma membrane of Gram-negative bacteria; PL^{G+}, phospholipid mixture mimicking the plasma membrane of Gram-positive bacteria; R_{EX}, exchange contribution to the transverse relaxation rate; R_H, hydrodynamic Stokes radius; SUV, small unilamellar vesicles; TM, transmembrane; TROSY, transverse relaxation-optimized spectroscopy.

REFERENCES

(1) Zasloff, M. (2002) Antimicrobial peptides of multicellular organisms. *Nature 415*, 389–395.

(2) Brown, K. L., and Hancock, R. E. (2006) Cationic host defense (antimicrobial) peptides. *Curr. Opin. Immunol. 18*, 24–30.

(3) Bulet, P., Stöcklin, R., and Menin, L. (2004) Anti-microbial peptides: From invertebrates to vertebrates. *Immunol. Rev. 198*, 169–184.

(4) Fahrner, R. L., Dieckmann, T., Harwig, S. S., Lehrer, R. I., Eisenberg, D., and Feigon, J. (1996) Solution structure of protegrin-1, a broad-spectrum antimicrobial peptide from porcine leukocytes. *Chem. Biol. 3*, 543–550.

(5) Kawano, K., Yoneya, T., Miyata, T., Yoshikawa, K., Tokunaga, F., Terada, Y., and Iwanaga, S. (1990) Antimicrobial peptide, tachyplesin I, isolated from hemocytes of the horseshoe crab (*Tachypleus tridentatus*). NMR determination of the β-sheet structure. *J. Biol. Chem. 265*, 15365–15367.

(6) Mandard, N., Bulet, P., Caille, A., Daffre, S., and Vovelle, F. (2002) The solution structure of gomesin, an antimicrobial cysteine-rich peptide from the spider. *Eur. J. Biochem. 269*, 1190–1198.

(7) Mandard, N., Sy, D., Maufrais, C., Bonmatin, J. M., Bulet, P., Hetru, C., and Vovelle, F. (1999) Androctonin, a novel antimicrobial peptide from scorpion *Androctonus australis*: Solution structure and molecular dynamics simulations in the presence of a lipid monolayer. *J. Biomol. Struct. Dyn. 17*, 367–380.

(8) Hancock, R. E., and Rozek, A. (2002) Role of membranes in the activities of antimicrobial cationic peptides. *FEMS Microbiol. Lett. 206*, 143–149.

(9) Fernandez, D. I., Gehman, J. D., and Separovic, F. (2009) Membrane interactions of antimicrobial peptides from Australian frogs. *Biochim. Biophys. Acta 1788*, 1630–1638.

(10) Baumann, G., and Mueller, P. (1974) A molecular model of membrane excitability. *J. Supramol. Struct. 2*, 538–557.

(11) Matsuzaki, K., Murase, O., Fujii, N., and Miyajima, K. (1996) An antimicrobial peptide, magainin 2, induced rapid flip-flop of phospholipids coupled with pore formation and peptide translocation. *Biochemistry 35*, 11361–11368.

(12) Ludtke, S. J., He, K., Heller, W. T., Harroun, T. A., Yang, L., and Huang, H. W. (1996) Membrane pores induced by magainin. *Biochemistry 35*, 13723–13728.

(13) Shai, Y. (1999) Mechanism of the binding, insertion and destabilization of phospholipid bilayer membranes by α-helical antimicrobial and cell non-selective membrane-lytic peptides. *Biochim. Biophys. Acta 1462*, 55–70.

(14) Bechinger, B. (2009) Rationalizing the membrane interactions of cationic amphipathic antimicrobial peptides by their molecular shape. *Curr. Opin. Colloid Interface Sci. 14*, 349–355.

(15) Brogden, K. A. (2005) Antimicrobial peptides: Pore formers or metabolic inhibitors in bacteria?. *Nat. Rev. Microbiol. 3*, 238–250.

(16) Ovchinnikova, T. V., Aleshina, G. M., Balandin, S. V., Krasnosdembskaya, A. D., Markelov, M. L., Frolova, E. I., Leonova, Y. F., Tagaev, A. A., Krasnodembsky, E. G., and Kokryakov, V. N. (2004) Purification and primary structure of two isoforms of arenicin, a novel antimicrobial peptide from marine polychaeta *Arenicola marina*. *FEBS Lett. 577*, 209–214.

(17) Ovchinnikova, T. V., Shenkarev, Z. O., Nadezhdin, K. D., Balandin, S. V., Zhmak, M. N., Kudelina, I. A., Finkina, E. I., Kokryakov, V. N., and Arseniev, A. S. (2007) Recombinant expression, synthesis, purification, and solution structure of arenicin. *Biochem. Biophys. Res. Commun. 360*, 156–162.

(18) Ovchinnikova, T. V., Shenkarev, Z. O., Balandin, S. V., Nadezhdin, K. D., Paramonov, A. S., Kokryakov, V. N., and Arseniev, A. S. (2008) Molecular insight into mechanism of antimicrobial action of the β-hairpin peptide arenicin: Specific oligomerization in detergent micelles. *Biopolymers 89*, 455–464.

(19) Cavanagh, J., Fairbrother, W. J., Palmer, A. G., III, Skelton, N. J. (1996) *Protein NMR Spectroscopy: Principles and Practice*, Academic Press, London.

(20) Delaglio, F., Wu, Z., and Bax, A. (2001) Measurement of homonuclear proton couplings from regular 2D COSY spectra. *J. Magn. Reson. 149*, 276–281.

(21) Güntert, P. (2004) Automated NMR structure calculation with CYANA. *Methods Mol. Biol. 278*, 353–378.

(22) Korzhnev, D. M., Billeter, M., Arseniev, A. S., and Orekhov, V. Y. (2001) NMR studies of Brownian tumbling and internal motions in proteins. *Prog. NMR Spectrosc. 38*, 197–266.

(23) Chill, J. H., Louis, J. M., Baber, J. L., and Bax, A. (2006) Measurement of ^{15}N relaxation in the detergent-solubilized tetrameric KcsA potassium channel. *J. Biomol. NMR. 36*, 123–136.

(24) Kneller, J. M., Lu, M., and Bracken, C. (2002) An effective method for the discrimination of motional anisotropy and chemical exchange. *J. Am. Chem. Soc. 124*, 1852–1853.

(25) Cole, R., and Loria, J. P. (2003) FAST-Modelfree: A program for rapid automated analysis of solution NMR spin-relaxation data. *J. Biomol. NMR 26*, 203–213.

(26) Battiste, J. L., and Wagner, G. (2000) Utilization of site-directed spin labeling and high-resolution heteronuclear nuclear magnetic resonance for global fold determination of large proteins with limited nuclear Overhauser effect data. *Biochemistry 39*, 5355–5365.

(27) Barsukov, L. I., Kulikov, V. I., and Bergelson, L. D. (1976) Lipid transfer proteins as a tool in the study of membrane structure. Inside-outside distribution of the phospholipids in the protoplasmic membrane of *Micrococcus lysodeikticus*. *Biochem. Biophys. Res. Commun. 71*, 704–711.

(28) Mueller, P., Rudin, D. O., Tien, H. T., and Wescott, W. C. (1962) Reconstitution of cell membrane structure in vitro and its transformation into an excitable system. *Nature 194*, 979–980.

(29) Stavrakoudis, A., Tsoulos, I. G., Shenkarev, Z. O., and Ovchinnikova, T. V. (2009) Molecular dynamics simulation of antimicrobial peptide arenicin-2: β-Hairpin stabilization by noncovalent interactions. *Biopolymers 92*, 143–155.

(30) Efremov, R. G., and Alix, A. J. (1993) Environmental characteristics of residues in proteins: Three-dimensional molecular hydrophobicity potential approach. *J. Biomol. Struct. Dyn. 11*, 483–507.

(31) Koradi, R., Billeter, M., and Wuthrich, K. (1996) MolMol: A program for display and analysis of macromolecular structures. *J. Mol. Graphics 14*, 51–55.

(32) Lee, D., Hilty, C., Wider, G., and Wüthrich, K. (2006) Effective rotational correlation times of proteins from NMR relaxation interference. *J. Magn. Reson. 178*, 72–76.

(33) Brown, L. R., Bosch, C., and Wuthrich, K. (1981) Location and orientation relative to the micelle surface for glucagon in mixed micelles with dodecylphosphocholine: EPR and NMR studies. *Biochim. Biophys. Acta 642*, 296–312.

(34) Buffy, J. J., Hong, T., Yamaguchi, S., Waring, A. J., Lehrer, R. I., and Hong, M. (2003) Solid-state NMR investigation of the depth of insertion of protegrin-1 in lipid bilayers using paramagnetic Mn^{2+}. *Biophys. J. 85*, 2363–2373.

(35) Kahn, P. C. (1979) The interpretation of near-ultraviolet circular dichroism. *Methods Enzymol. 61*, 339–378.

(36) Andrä, J., Hammer, M. U., Grötzinger, J., Jakovkin, I., Lindner, B., Vollmer, E., Fedders, H., Leippe, M., and Gutsmann, T. (2009) *Biol. Chem. 390*, 337–349.

(37) Andrä, J., Goldmann, T., Ernst, C. M., Peschel, A., and Gutsmann, T. (2011) Multiple peptide resistance factor (MPRF)-mediated resistance of *Staphylococcus aureus* against antimicrobial peptides coincides with a modulated peptide interaction with artificial membranes comprising lysylphosphatidylglycerol. *J. Biol. Chem. 286*, 18692–18700.

(38) Andrä, J., Jakovkin, I., Grötzinger, J., Hecht, O., Krasnosdembskaya, A. D., Goldmann, T., Gutsmann, T., and Leippe, M. (2008) Significance of the cyclic structure and of arginine residues for the antibacterial activity of arenicin-1 and its interaction with phospholipid and lipopolysaccharide model membranes. *Biochem. J. 410*, 113–122.

(39) Sanders, C. R., and Sonnichsen, F. (2006) Solution NMR of membrane proteins: Practice and challenges. *Magn. Reson. Chem. 44*, S24–S40.

(40) Salnikov, E. S., Aisenbrey, C., Balandin, S. V., Zhmak, M. N., Ovchinnikova, T. V., and Bechinger, B. (2011) Structure and alignment of the membrane-associated antimicrobial peptide arenicin by oriented solid-state NMR spectroscopy. *Biochemistry 50*, 3784–3795.

(41) Haney, E. F., Hunter, H. N., Matsuzaki, K., and Vogel, H. J. (2009) Solution NMR studies of amphibian antimicrobial peptides: Linking structure to function?. *Biochim. Biophys. Acta 1788*, 1639–1655.

(42) Porcelli, F., Buck-Koehntop, B. A., Thennarasu, S., Ramamoorthy, A., and Veglia, G. (2006) Structures of the dimeric and monomeric variants of magainin antimicrobial peptides (MSI-78 and MSI-594) in micelles and bilayers, determined by NMR spectroscopy. *Biochemistry 45*, 5793–5799.

(43) Saravanan, R., and Bhattacharjya, S. (2011) Oligomeric structure of a cathelicidin antimicrobial peptide in dodecylphosphocholine micelle determined by NMR spectroscopy. *Biochim. Biophys. Acta 1808*, 369–381.

(44) Laederach, A., Andreotti, A. H., and Fulton, D. B. (2002) Solution and micelle-bound structures of tachyplesin I and its active aromatic linear derivatives. *Biochemistry 41*, 12359–12368.

(45) Doherty, T., Waring, A. J., and Hong, M. (2006) Membrane-bound conformation and topology of the antimicrobial peptide tachyplesin I by solid-state NMR. *Biochemistry 45*, 13323–13330.

(46) Powers, J. P., Tan, A., Ramamoorthy, A., and Hancock, R. E. (2005) Solution structure and interaction of the antimicrobial polyphemusins with lipid membranes. *Biochemistry 44*, 15504–15513.

(47) Mani, R., Cady, S. D., Tang, M., Waring, A. J., Lehrer, R. I., and Hong, M. (2006) Membrane-dependent oligomeric structure and pore formation of a β-hairpin antimicrobial peptide in lipid bilayers from solid-state NMR. *Proc. Natl. Acad. Sci. U.S.A. 103*, 16242–16247.

(48) Tang, M., Waring, A. J., and Hong, M. (2007) Phosphate-mediated arginine insertion into lipid membranes and pore formation by a cationic membrane peptide from solid-state NMR. *J. Am. Chem. Soc. 129*, 11438–11446.

(49) Sansom, M. S. (1991) The biophysics of peptide models of ion channels. *Prog. Biophys. Mol. Biol. 55*, 139–235.

(50) Huang, H. W. (2006) Molecular mechanism of antimicrobial peptides: The origin of cooperativity. *Biochim. Biophys. Acta 1758*, 1292–1302.

(51) Salnikov, E., Aisenbrey, C., Vidovic, V., and Bechinger, B. (2010) Solid-state NMR approaches to measure topological equilibria and dynamics of membrane polypeptides. *Biochim. Biophys. Acta 1798*, 258–265.